PRESSURE TREATMENT OF METALS

Regularities of Formation and Degradation of the Microstructure and Properties of New Ultrafine-Grained Low-Modulus Ti–Nb–Mo–Zr Alloys

Yu. R. Kolobov[a, c], *, O. A. Golosova[b], **, and S. S. Manokhin[c], ***

[a]*Belgorod State National Research University, Belgorod, 308034 Russia*
[b]*Merzhanov Institute of Structural Macrokinetics and Materials Science, Russian Academy of Sciences, Chernogolovka, Moscow oblast, 142432 Russia*
[c]*Institute of Problems of Chemical Physics, Russian Academy of Sciences, Chernogolovka, Moscow oblast, 142432 Russia*
*e-mail: kolobov@bsu.edu.ru
**e-mail: golosova@ism.ac.ru
***e-mail: manohin@bk.ru
Received October 2, 2017; in final form, November 7, 2017; accepted for publication November 10, 2017

Abstract—Regularities of the formation of ultrafine-grained (UFG) and submicrocrystalline (SMC) structures in new nickel-free low-modulus Ti–Nb–Mo–Zr titanium β alloys under the action of plastic deformation have been studied. Temperature–time ranges of the development of dynamic recrystallization processes under the simultaneous action of temperature and plastic deformation are determined. A type-II recrystallization diagram of the Ti–28Nb–8Mo–12Zr alloy is constructed and analyzed. It is shown using scanning electron microscopy and the electron backscatter diffraction method that the UFG structure with an average grain size of no more than 7 μm and high fraction of high-angle grain boundaries is formed in the investigated alloys as a result of longitudinal rolling, followed by annealing for quenching. It is found that the formation of the UFG structure leads to a significant increase in the strength and plastic characteristics of these alloys. The regularities of the formation of UFG and SMC structures in titanium β alloys Ti–28Nb–8Mo–12Zr and industrial VT30 under the action of plastic deformation by the helical rolling method are studied. It is shown that the helical rolling of the VT30 alloy leads to the formation of the homogeneous UFG state as opposed to the Ti–28Nb–8Mo–12Zr alloy, where this method causes structure softening with micropores and microcracks formed in the central region. It is possible to form a nanostructured state with an average grain size of about 100 nm in Ti–Nb–Mo–Zr titanium β alloys using the high-pressure torsion method.

Keywords: low-modulus titanium alloy, ultrafine-grained structure, nanostructured state, mechanical properties, helical rolling, severe plastic deformation

DOI: 10.3103/S1067821218040090

INTRODUCTION

Demand for medical implants in various fields of medicine (maxillofacial surgery, stomatology, orthopedics, traumatology, etc.) is increasing. Despite the long-standing predictions for a reduction in the use of non-biodegradable metallic implants and endoprostheses as medical products of the considered application, titanium and its alloys remain the most suitable materials for the manufacture of bone medical implants and others. Such biomaterials need enhanced biochemical and biomechanical compatibility with a living body and improvement strength and reliability [1–5]. In this regard, scientific research and innovative developments making it possible to create the implants and materials for their production with improved performance are relevant.

The wide use of titanium and it alloys to manufacture implants and endoprostheses is caused by the unique combination of their properties: high strength, light weight, and low elastic modulus. Metallic materials of biomedical application including Ti alloys should possess biochemical compatibility with body tissues (a lack of immune reactions and inflammatory processes) and biomechanical compatibility, which determines the functional reliability of implants [1, 6–8]. The main characteristic of the biomechanical compatibility of an implanted material is the elastic modulus. It is desirable to achieve an elastic modulus close to that corresponding to bone tissue ($E = 30–35$ GPa) [9–11]. This makes it possible to redistribute a significant part of loads between the bone and the implant so that the bone/implant system functions as a natural composite [5, 12, 13]. From this

viewpoint, titanium β alloys with low elastic modulus close to that for bone tissue and, accordingly, providing biomechanical compatibility, are the most promising for wide use as a material for implantology. Biomechanical compatibility means a minimum degree or absence of overloads and microshifts at the implant/tissue interface. To achieve full biocompatibility, it is necessary to used implants made from low-modulus materials containing no elements harmful to a living body [7, 14]. In addition, superelasticity and shape memory effect are also important for these materials. These materials—Ti−Nb [15, 16], Ti−Nb−Zr(Ta) [17], Ti−Nb−Ta−Zr [18−20], Ti−Nb−Hf−Zr [21], and Ti−Nb−Sn [22, 23] β alloys—demonstrate a shape memory effect depending on their thermomechanical treatment or the content of alloying elements. However, a decrease in the elastic modulus owing to the application of various alloying systems (taking into account the use of β stabilizers having no harmful effect on the living body) favors the deterioration of strength characteristics. This requires searching for methods to improve properties while retaining low elastic modulus.

One of the approaches developed in recent years to achieve high strength properties in metals and alloys is the formation of ultrafine-grained (UFG), submicrocrystalline (SMC), or nanostructured (NC) states by the action of plastic deformation. According to the terminology adopted in the 1980s, UFG materials include metals and alloys with a grain size in the range of 1−10 μm, SMC materials are materials with a grain size of 0.1−1 μm, and the grain size in the NS materials is less than 100 nm (this is accepted in recent decades in the period of extensive development of nanotechnology and nanomaterials) [1]. It is known that the formation of these structures in metals and alloys, including in titanium β alloys, leads to a significant improvement in their mechanical properties, including those necessary for use as materials for medical implants [1, 24−26]. For example, the shape-memory β alloys Ti−19.7Nb−5.8Ta [27] and Ti−24Nb−4Zr−8Sn [28] and β alloys Ti−15Mo [29−31] and Ti−29Nb−13Ta−4.6Zr [32] with SMC and NS states formed under the action of plastic deformation, including severe plastic deformation, are characterized by high strength characteristics and microhardness.

New titanium β alloys of the Ti−Nb−Mo−Zr system were developed as a result of the collaboration of the Belgorod State National Research University with CRISM Prometei (St. Petersburg) and melted at the production center of the VSMPO-AVISMA Corporation (Verkhnyaya Salda, Russia). Theoretical calculation and analysis of the choice of the chemical composition of new titanium Ti−Nb−Mo−Zr alloys are presented in [33].

Literature data available on the study of titanium β alloys with a similar alloying system make it possible only to predict the level of properties, inasmuch as there are no complex studies of regularities of the formation of the structure and properties of the alloys under consideration with the indicated alloying system both in Russia and abroad. In this context, the study of regularities of the formation and degradation of the microstructure and properties of new ultrafine-grained low-modulus alloys Ti−Nb−Mo−Zr has attracted a high degree of interest. In this paper, we present a review of the results of original research by the authors, including those described in previously published papers [33−36].

REGULARITIES OF THE FORMATION AND DEGRADATION OF A UFG STRUCTURE IN TITANIUM ALLOYS UNDER THE ACTION OF PLASTIC DEFORMATION

To study the regularities of the formation of the microstructure under conditions of the action of plastic deformation, we chose new titanium β alloys with different degrees of alloying: Ti−19Nb−7Mo−14Zr and Ti−28Nb−8Mo−12Zr [33−36]. These alloys, after casting followed by forging (the initial state), are represented only by the β phase and exhibit a uniform coarse-grained structure with an average grain size of ~250 and ~350 μm, respectively (Fig. 1).

To reveal regularities of the formation of the UFG structure as a result of the development of recrystallization processes, a diagram of recrystallization of type II was constructed based on metallographic studies of the Ti−28Nb−8Mo−12Zr alloy as an example after uniaxial upsetting with various degrees of deformations (30, 50, and 70%) at temperatures of 700, 800, and 900°C. This shows the dependence between grain size, degree of deformation, and annealing temperature (Fig. 2). This made it possible to predict temperature and time conditions of the formation of the UFG structure, which is controlled by the development of dynamic recrystallization processes upon hot deformation.

Figure 3a shows the microstructure of Ti−28Nb−8Mo−12Zr alloy samples after upsetting. It is seen that at, $t = 700°C$, no development of the recrystallization processes is observed. Inside the initial coarse grains, a network of the grain boundaries, which are apparently low-angle grain boundaries, is formed. This indicates the development of the dynamic polygonization processes with the formation of low-angle subboundaries and is confirmed by the electron backscatter diffraction (EBSD) analysis data.

The increase in the deformation temperature to 800°C leads to the appearance of new fine grains along the initial high-angle grain boundaries as a result of the development of the dynamic recrystallization processes. It should be noted that the recrystallization nuclei are formed predominantly at the nonequilibrium triple junctions of grains, around which there is
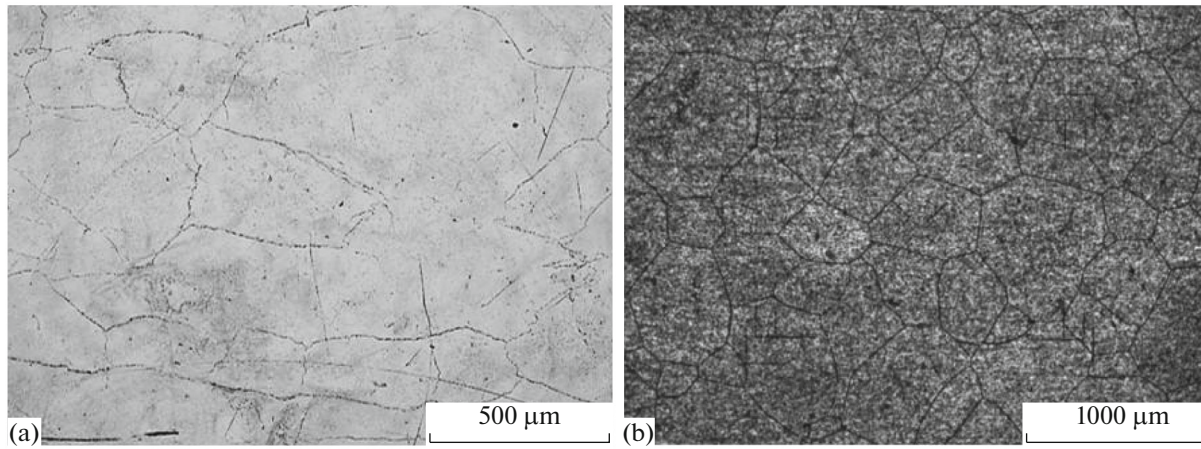
Fig. 1. Microstructure of the (a) Ti−19Nb−7Mo−14Zr and (b) Ti−28Nb−8Mo−12Zr alloys in the initial coarse-grained state. Optical metallography.

an increased curvature of grain boundaries. The state after deformation with $\varepsilon = 30\%$ is characterized by the lowest average size of recrystallized grains $d \sim 17~\mu m$. The volume fraction of recrystallized grains is only ~1%. The further formation and growth of grains occur consequentially along the grain boundaries from the triple junction (Fig. 3b). With an increase in the degree of deformation to 70%, the average size of recrystallized grains reaches ~20 μm and their volume fraction increases to 5.5%. Upon a further increase in the deformation temperature to 900°C, the fine recrystallized grains growing owing to the coarse deformed ones occupy a much greater bulk. The average size of recrystallized grains is seen in Fig. 3c to increase more than 2 times. The recrystallization diagram shows (Fig. 2) that the average size of deformed grains decreases substantially with increasing upsetting temperature. The volume fraction of recrystallized grains in the state with the lowest degree of deformation at this temperature does not exceed 3%. The further increase in the degree of deformation to 50% leads to a sharp growth in these grains (to 17 vol %). In the state with maximum degree of deformation, the volume fraction of the recrystallization regions is 23%. The data on the temperature and time ranges of the development of the dynamic recrystallization processes were used to determine the optimal conditions of formation of the UFG structure in low-modulus titanium alloys upon longitudinal and helical rolling. Earlier, the authors developed pilot industrial technology to produce nanostructured titanium for medical application using helical rolling [25].

Helical rolling made it possible to form UFG and SMC states in the low-modulus titanium alloy Ti−11.5Mo−6Zr−4.5Sn (VT30) with an average grain size of ~12 μm. The VT30 alloy was used as a model one, and this choice is caused by the well-described technological regimes of its treatment and its sufficiently high plasticity. The process of the helical rolling of the VT30 alloy was carried out in a pass from a diameter of 16 to 9 mm at temperatures of 500, 600, and 700°C and different rolling rates. The rotation rate of rolls was regulated using frequency converters by the change in the frequency of the applied current.

Helical rolling with the degree of deformation $\varepsilon = 44\%$ substantially affects the structural and phase state of the titanium β alloy VT30. It is found that a decrease in the grain size during helical rolling is accompanied by a change in the phase state. In the structure of the material, the precipitation of the α phase is observed. This feature was revealed only in the case of rolling with the lowest rate ($v \sim 16$ mm/s). This effect of the deformation initiation of the phase transformation and the precipitation of the α phase is detected for
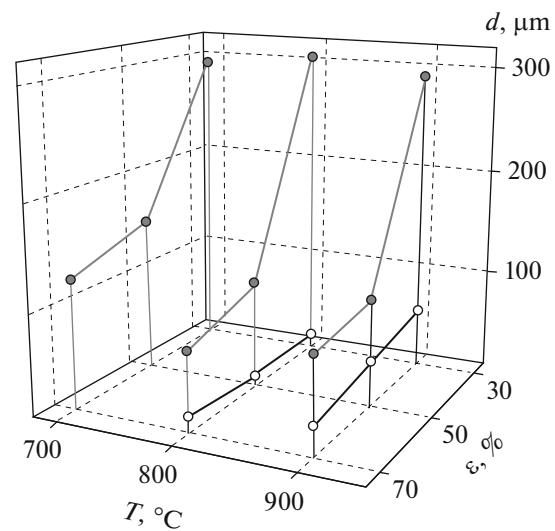
Fig. 2. Recrystallization diagram of type II of the Ti−28Nb−8Mo−12Zr alloy. (−•−) coarse deformed and recrystallized grains; (−○−) recrystallized grains.
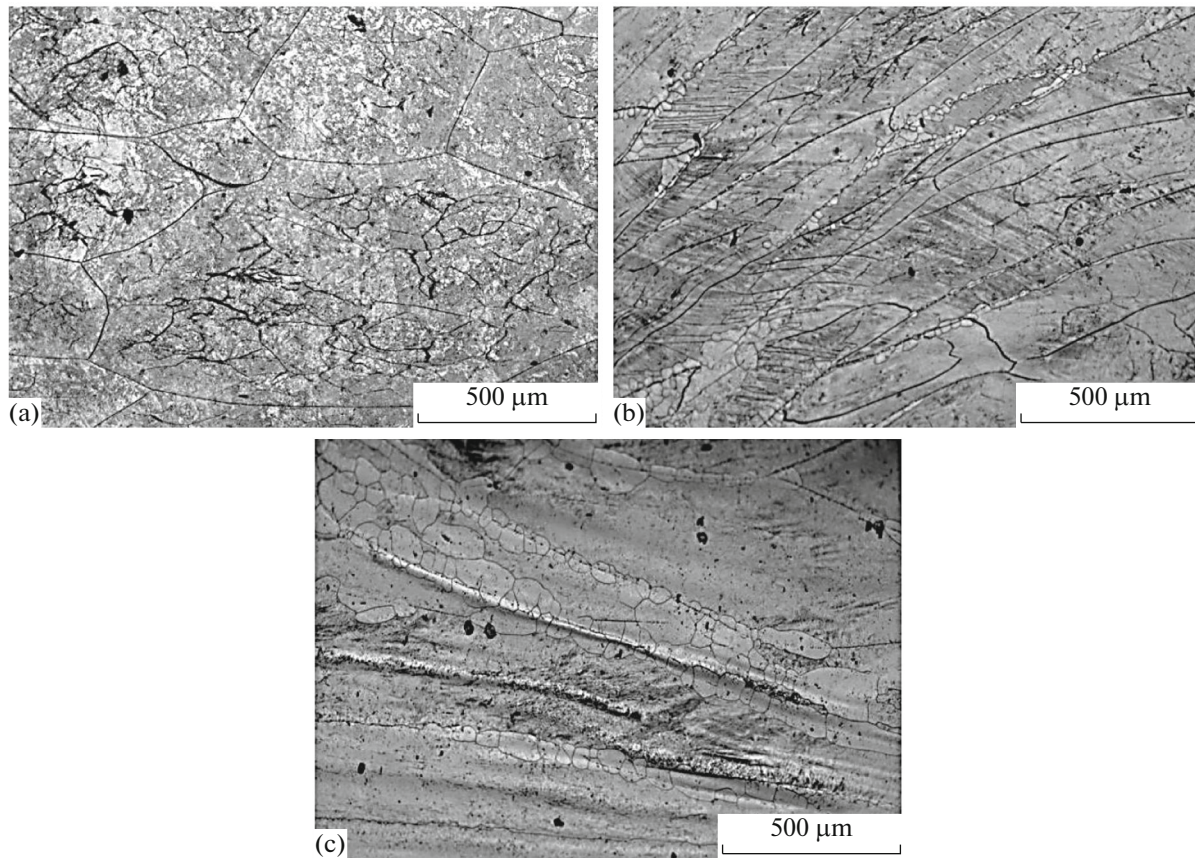
Fig. 3. Microstructure of the Ti−28Nb−8Mo−12Zr alloy after upsetting at various temperatures and degrees of deformation. *t*, °C: (a) 700, (b) 800, (c) 900. ε, %: (a) 30, (b) 50, (c) 70.

all three temperatures. As this takes place, the volume fraction of the α phase increases from 6 to 12% with increasing rolling temperature.

Figure 4 shows the microstructure of the VT30 alloy after helical rolling at *t* = 700°C, where the α phase represent dark regions. At this temperature, the decomposition of the β phase occurs over the entire section of the rods. The volume fraction of the α phase is substantially smaller in the central part of the rod than that at the periphery characterized by the higher degree of shear deformation. In the peripheral region, the average β grain size is about 0.3 μm.

With increasing rolling rate (to *v* ~ 40 mm/s), no α phase is formed in the VT30 alloy. Helical rolling with this rate at *t* = 500 and 600°C favors the formation of an inhomogeneous microstructure over the entire section of rod. In the rod center, the coarse initial deformed grains elongated along the rolling direction with a partially fragmented internal structure are observed. The globular SMC structure with an average grain size of ~0.8 μm is formed at the periphery.

Upon increase in the rolling temperature to 700°C, a recrystallized homogeneous UFG state with an average grain size of ~1 μm is formed in the investigated VT30 alloy (Fig. 5).

These data indicate that the helical rolling is an effective method to form the UFG state in the titanium β alloy using the example of Ti−11.5Mo−6Zr−4.5Sn (VT30). However, in the case of the Ti−28Nb−8Mo−12Zr alloy under consideration, a homogeneous UFG structure is not formed. The equiaxed dynamically recrystallized UFG structure is formed only at the periphery. The average grain size is ~2 μm. In the central part of the rod, there is almost no refinement of the structure; the initial deformed (elongated along the rolling direction) grains and pores are observed.

The increase in the rolling temperature to 950°C and degree of deformation to 55% favors no formation of the uniform UFG structure in this alloy. In the central part, micropores and microcraks are also observed (Fig. 6a). It can be seen in Fig. 6b that, in this state, when compared to the previous one, there are coarse (several tens of micrometers) recrystallized regions characterized by a grain size of 3 μm. The volume fraction of these regions in the center is insignificant; the coarse grains elongated along the rolling direction (rod axis) with a fragmented structure prevail.
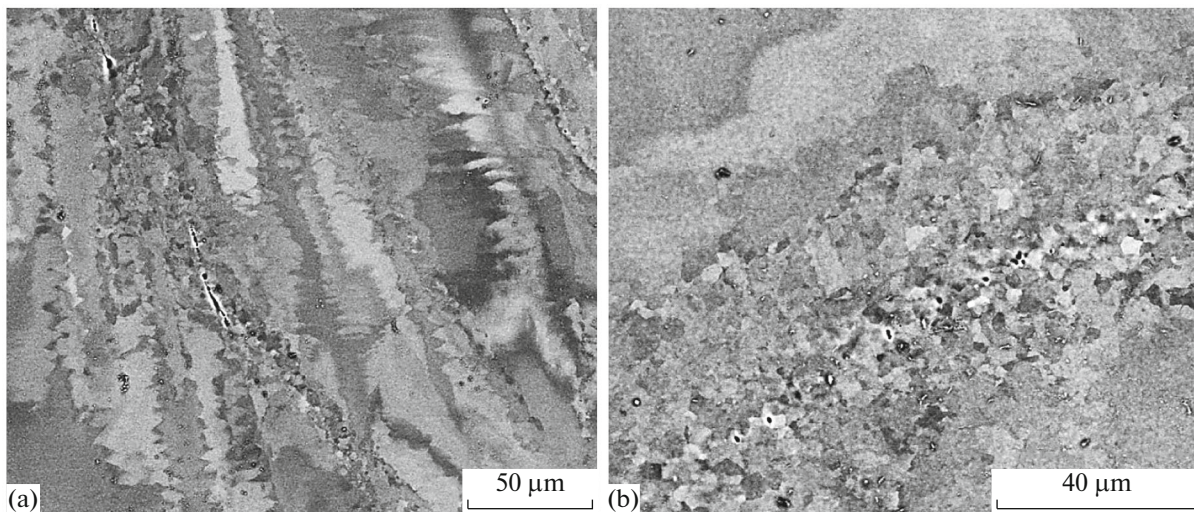
Thus, these data do not allow us to consider this method to be a promising one to form UFG and SMC states in titanium alloys Ti−Nb−Mo−Zr.
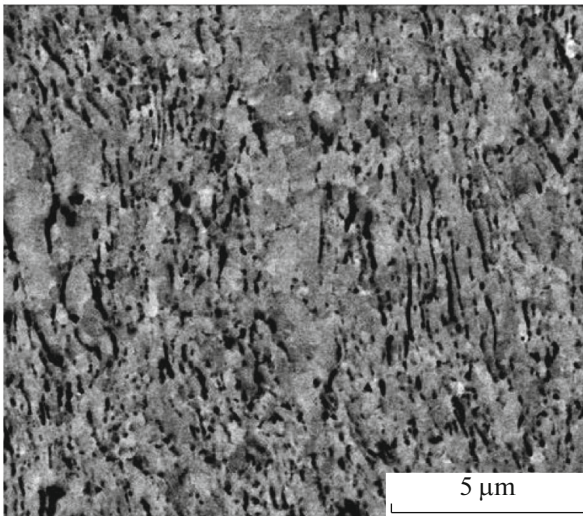
Fig. 4. SEM image of the Ti–11.5Mo–6Zr–4.5Sn alloy after helical rolling at $t = 700°C$ and $v \sim 16$ mm/s (periphery).
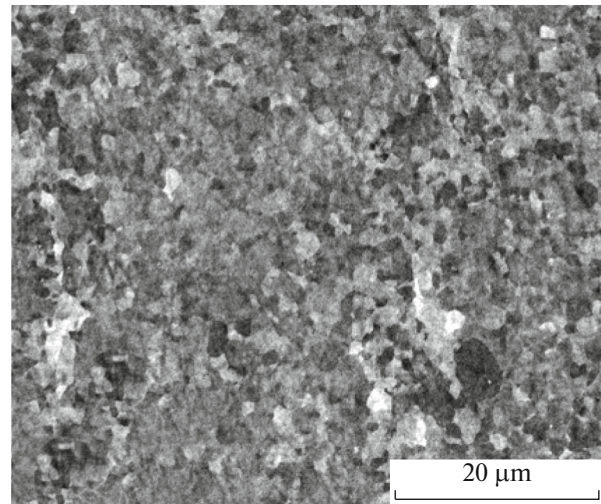
Fig. 5. SEM image of the Ti–11.5Mo–6Zr–4.5Sn alloy after helical rolling at $t = 700°C$ and $v \sim 40$ mm/s (center).
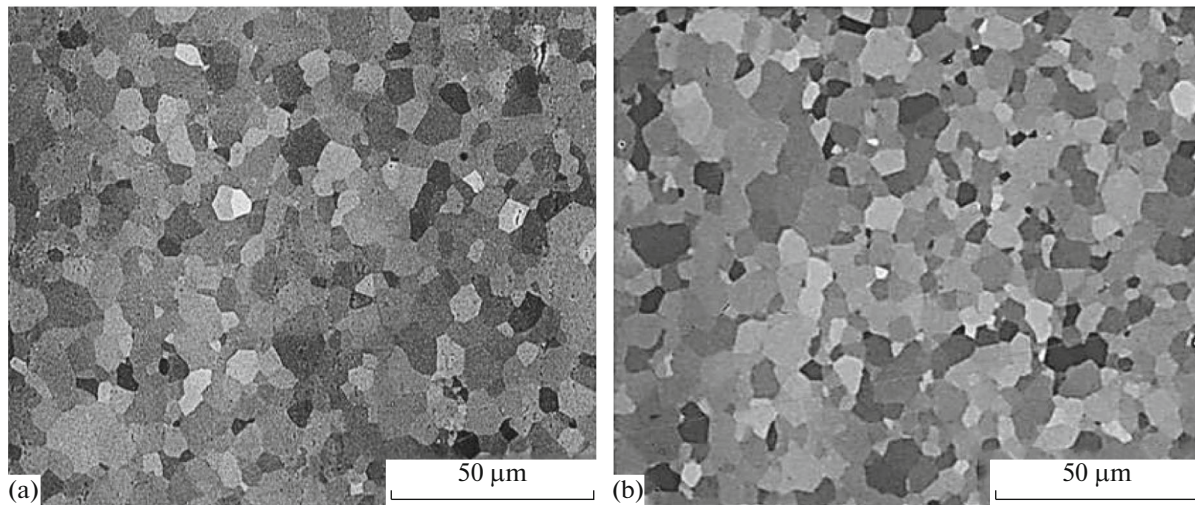

Fig. 6. SEM images of the Ti–28Nb–8Mo–12Zr alloy after helical rolling at $t = 950°C$ and $v \sim 40$ mm/s (center).

To study the regularities of formation of the UFG state, longitudinal rolling with a degree of accumulated deformation of 60% at $t = 700°C$ followed by annealing for quenching at $t = 700$ and $800°C$ was used. As a result of the indicated treatment in the Ti–19Nb–7Mo–14Zr and Ti–28Nb–8Mo–12Zr alloys, the homogeneous equiaxed UFG state with an average grain size of 4.5 and 6.5 μm, respectively, is formed (Fig. 7). The fraction of the high-angle grain boundaries in these titanium alloys is about the same; it is 91% for Ti–19Nb–7Mo–14Zr and 87% for Ti–28Nb–8Mo–12Zr. In [33–35], we showed, using the example of the Ti–26Nb–7Mo–12Zr alloy, the possibility of formation of the homogeneous globular UFG structure with an average grain size of 9 μm and high fraction of high-angle grain boundaries under conditions of static recrystallization development after cold sheet rolling and subsequent high-temperature annealing.

The study of the fine structure using transmission electron microscopy (TEM) showed (Fig. 8) that the grains of the Ti–19Nb–7Mo–14Zr and Ti–28Nb–8Mo–12Zr alloys have a fine banded substructure, which is not revealed by scanning electron microscopy (SEM) or the EBSD method. The width of bands observed clearly in the regime of transmission scanning electron microscopy (TSEM) is in the range of 20–500 nm (Fig. 8a). Figure 8b shows that the orien-

Fig. 7. Microstructure of the (a) Ti−19Nb−7Mo−14Zr and (b) Ti−28Nb−8Mo−12Zr alloys after longitudinal rolling at $t = 700°C$ and subsequent annealing for quenching.
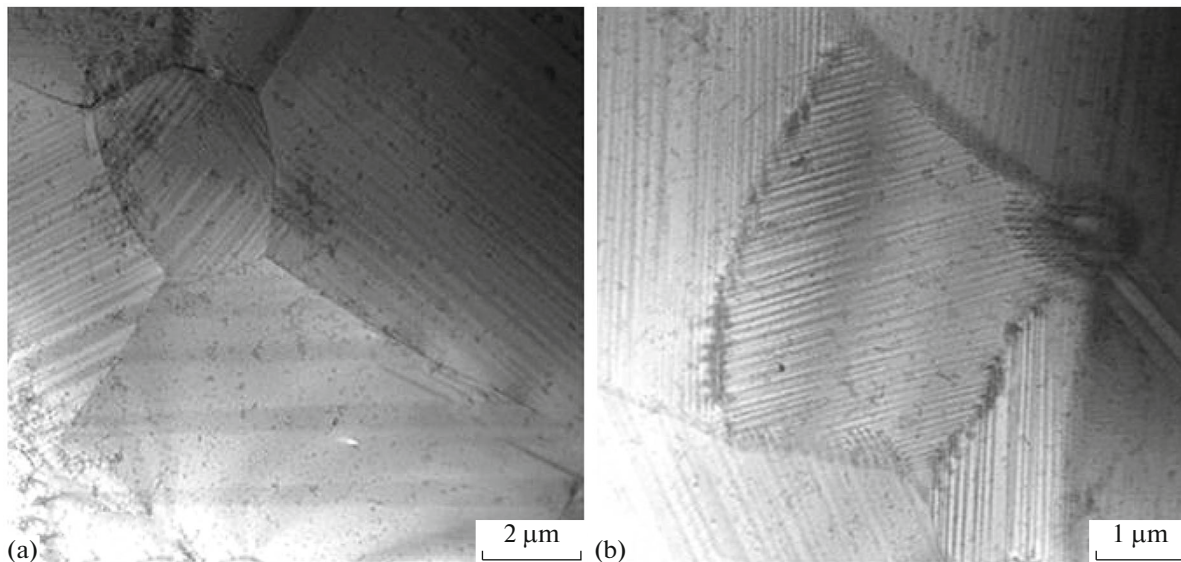

Fig. 8. TSEM images of the Ti−28Nb−8Mo−12Zr alloy after longitudinal rolling at $t = 700°C$ and subsequent annealing for quenching at $t = 800°C$.

tation of an intragranular banded structure in various grains differs. This is caused by the connection of the banded structure with crystallographic orientation. The formation of the fine banded structure can be explained by the phase instability of the bcc β phase upon quenching after recrystallized annealing. Forming fine interlayers of the martensitic phase (α″ martensite) are not detected by the diffraction method because of a low reflected ability. However, these interlayers create a field of stresses in the material, which is close to the periodic field corresponding to the period of the banded structure. In addition, the α″ phase has a different volume per atom and, accord-

ingly, density from β phase. Thus, the α″ phase is easily detected using a TSEM contrast with the registration of high-angle transmission electrons.

FORMATION OF A NANOSTRUCTURED STATE IN NEW LOW-MODULUS TITANIUM ALLOYS UNDER THE ACTION OF SEVERE PLASTIC DEFORMATION

The formation of SMC or NS states in titanium alloys under investigation to improve mechanical properties while retaining the low elastic modulus is of the greatest interest. In the present paper, we used the
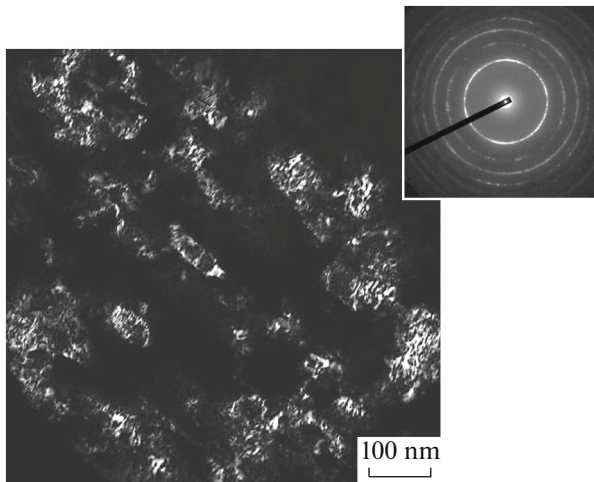
Fig. 9. Dark-field image and electron-diffraction pattern of the Ti−19Nb−7Mo−14Zr alloy after high-pressure torsion.

high-pressure torsion (HPT) method to produce SMC and NS states in titanium β alloys. The samples (7 mm diameter and 2.2 mm thick) were cut from a UFG rod fabricated by longitudinal rolling and subsequent annealing. As a result of HPT (number of revolutions $n = 5$, $P = 5$ GPa) at room temperature, disklike samples of the investigated alloy with a diameter of 10 mm and thickness of 0.8 mm were produced.

In the Ti−19Nb−7Mo−14Zr sample processed by HPT with a degree of true strain $\varepsilon_t = 3.6$, the NS state is formed at the periphery (Fig. 9). The element size of the grain−subgrain structure lies within the range of 50−150 μm. The electron-diffraction pattern for an area of ~1.3 μm² shows the quasi-ring character of the location of reflections, which indicates a great number of grains in this area and, accordingly, the nanostructured state.

The subsequent annealing at $t = 550°$C contributes to an increase in the average size of elements of the grain−subgrain structure to about 125 nm (Fig. 10a). With further increasing annealing temperature, there is a substantial growth of grains as a result of the development of the recrystallization processes. Note that the grains, like in the case of the UFG state of this alloy, have a banded substructure caused by the presence of the α'' phase (Fig. 10b).

It is worth noting that the character of the structure produced in the Ti−28Nb−8Mo−12Zr alloy with the greatest concentration of alloying elements by the action of HPT corresponds to that formed in the case of the Ti−19Nb−7Mo−14Zr alloy. In the Ti−28Nb−8Mo−12Zr alloy after HPT and annealing at $t = 600°$C, the processes of recrystallization with the formation of the homogeneous SMC state with an average grain size of 900 nm are actively developed.

MECHANICAL PROPERTIES AND ELASTIC MODULUS OF NEW LOW-MODULUS TITANIUM ALLOYS

The results of mechanical tensile tests (Table 1) show that the developed new biomaterials belong to the class of titanium alloy with medium strength ($\sigma_u = 750-1000$ MPa) [33, 35], which also includes titanium alloy VT6 [37]. However, the alloys under consideration unfortunately possess low plasticity (δ), determined as the maximum elongation before failure. For
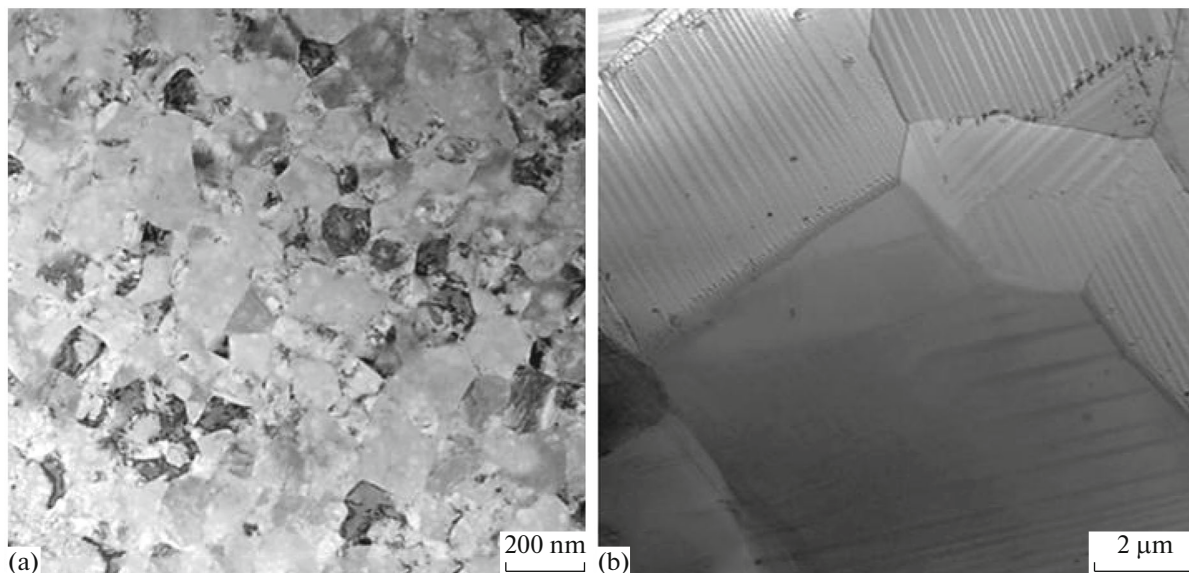
Fig. 10. TSEM images of the Ti−19Nb−7Mo−14Zr alloy after high-pressure torsion followed by annealing for quenching at $t = 550°$C.

Table 1. Mechanical properties of titanium β alloys in the initial coarse-grained (CG), fine-grained (FG), and ultrafine-grained (UFG) states

Alloy	State	$\sigma_{0.2}$, MPa	σ_u, MPa	δ, %	E, GPa
Ti–19Nb–7Mo–14Zr	CG	802 ± 31	806 ± 28	3.4 ± 0.7	71
	UFG (ε = 60%)	948 ± 2	958 ± 3	7.5 ± 0.6	69
Ti–28Nb–8Mo–12Zr	CG	650 ± 31	654 ± 23	2.4 ± 0.2	69
	UFG (ε = 60%)	792 ± 9	798 ± 7	16 ± 0.9	74
VT30	FG	941 ± 13	947 ± 12	7.3 ± 0.3	71
	UFG (ε = 55%)	979 ± 4	1009 ± 7	5.6 ± 0.4	76

Ti–28Nb–8Mo–12Zr alloy, δ is about ~2.5%. The production of the homogeneous globular UFG structure in the indicated alloys leads to a noticeable increase in the strength and plastic characteristic. The highest plasticity (about 16%) is reached in the UFG Ti–28Nb–8Mo–12Zr alloy. However, we showed in [34] that, upon the formation of the UFG structure in the Ti–26Nb–7Mo–12Zr alloy with a medium concentration of alloying elements using cold sheet rolling and subsequent recrystallized annealing, an insignificant decrease in the strength properties from 800 to 750 MPa takes place.

In the investigated alloys, the elastic modulus estimated from the slope of the elastic part of the stress-strain curve of samples in the initial coarse-grained state is E ~70 GPa and practically does not depend on the concentration of alloying elements (Table 1). The formation of the UFG structure in the Ti–19Nb–7Mo–14Zr alloy favors an insignificant decrease in the elastic modulus; its value somewhat increases in the Ti–28Nb–8Mo–12Zr alloy.

It should be noted that the formation of the UFG structure in the titanium β alloy VT30 leads to an increase in the strength characteristics and elastic modulus. However, at the same time, the plasticity changes insignificantly.

To estimate the mechanical properties of NS titanium alloys produced by HPT, the measurements of microhardness were carried out. The microhardness of the Ti–19Nb–7Mo–14Zr alloy in the NS state is ~450 HV, which is 140 HV higher than that in the UFG state (310 *HV*). It is known that the ratio of yield stress to microhardness is 3 : 1. It can be assumed based on this that the NS titanium β alloy Ti–19Nb–7Mo–14Zr exhibits a high yield stress of about 1200–1300 MPa. Thus, the formation of the NS state in the titanium β alloy Ti–Nb–Mo–Zr leads to a significant increase in the strength characteristics (~1.5 times) when compared to the UFG state. The analogous results are presented in [30–32]. In a Ti–15Mo β alloy with sufficiently low elastic modulus (93 GPa), the formation of the NS state by the HPT process results in an improvement in the strength properties; in particular, microhardness increases to 4200 MPa (~430 *HV*) [30, 31]. In the case of the widely known titanium β alloys Ti–29Nb–13Ta–4.6Zr of medical application, the NS state possesses increased characteristics (yield stress of ~800 MPa, ultimate tensile strength of ~1100 MPa, and hardness of ~300 *HV*) while retaining low elastic modulus (60 GPa) [32].

CONCLUSIONS

(1) Regularities and mechanisms of the formation of the homogeneous ultrafine-grained structure in low-modulus titanium alloys Ti–Nb–Mo–Zr are studied. It is found that the homogeneous UFG state with a high fraction of high-angle grain boundaries in the Ti–19Nb–7Mo–14Zr (average grain size d = 4.5 μm) and Ti–28Nb–8Mo–12Zr (d = 6.5 μm) alloys is formed by hot longitudinal rolling followed by annealing.

(2) It is shown that the formation of the ultrafine-grained structure (d ~ 1 μm) in the β alloys VT30 and Ti–28Nb–8Mo–12Zr under conditions of plastic deformation action by the helical rolling method is associated with the development of dynamic recrystallization processes. It is revealed that the formation of the UFG structure in these alloys leads both to an increase in the strength and plastic characteristics and to an insignificant increase in the elastic modulus (to ~75 GPa).

(3) It is found that the nanostructured state with an average grain size of d ~100 nm is formed in the titanium β alloys Ti–19Nb–7Mo–14Zr and Ti–28Nb–8Mo–12Zr as a result of the action of severe plastic deformation by high-pressure torsion.

(4) The use of newly developed titanium β alloys makes it possible to substantially decrease the elastic modulus (to 75 GPa) of the implanted material when compared to the titanium VT1–0 and VT6 alloys widely applied in medicine with an elastic modulus of 112 GPa.

REFERENCES

1. Kolobov, Yu.R., Nanotechnologies for the formation of medical implants based on titanium alloys with bioactive coatings, *Nanotechnol. Russ.*, 2009, vol. 4, nos. 11–12, pp. 758–775.

2. Stráskýa, J., Harcubaa, P., Václavováa, K., Horváth, K., Landa, M., Srba, O., and Janeček, M., Increasing strength of a biomedical Ti–Nb–Ta–Zr alloy by alloying with Fe, Si and O. *J. Mechan. Behav. Biomed. Mater.*, 2017, vol. 71, pp. 329–336.

3. Wong, J.Y. and Bronzino, J.D., *Biomaterials*, Boca Raton: CRC, Taylor & Francis, 2007.

4. Gunawarman, B., Niinomi, M., Akahori, T., Souma, T., Ikeda, M., and Tada, H., Mechanical properties and microstructure of low cost β-titanium alloys for healthcare applications. *Mater. Sci. Eng. C*, 2005, vol. 25, no. 3, pp. 304–311.

5. Geetha, M., Singh, A.K., Asokamani, R., and Gogia, A.K., Ti based biomaterials, the ultimate choice for orthopedic implants: A review, *Progr. Mater. Sci.*, 2009, vol. 54, pp. 397–425.

6. Yaszemski, M.J., Trantolo, D.J., Lewandrowski, K., and Hasirci, V., *Biomaterials in Orthopedics*, New York: Marcel Dekker, 2004.

7. Long, Marc and Rack, H.J., Titanium alloys in total joint replacement—material science perspective, *Biomaterials*, 1998, vol. 19, pp. 1621–1639.

8. Epple, M., *Biomaterialien und Biomineralisation*, Wiesbaden: Vieweg + Teubner, 2003.

9. Peterson, D.R. and Bronzino, J.D., *Biomechanics Principles and Applications*, Boca Raton: CRC, Taylor & Francis, 2008.

10. Niinomi, M., Nakai, M., and Heida J., Development of new metallic alloys for biomedical applications, *Acta Biomater.*, 2012, vol. 8, no. 11, pp. 3888–3903.

11. Leyens, C. and Peter, M., *Titanium and Titanium Alloys. Fundamentals and Applications*, Weinheim: Wiley, 2003.

12. Ranter, B.D., Hoffman, A.S., Schoen, F.J., and Lemons, J.E., *Biomaterials Science: An Introduction to Materials in Medicine*, San Diego: Elsevier, 2004, 2nd ed.

13. Hanawa, T., Hiromoto, S., and Yamamoto, A., Metallic biomaterials in body fluid and their surface modification, in *Structural Biomaterials for the 21 Century*, New Orleans: TMS, 2001, pp. 145–154.

14. Niinomi, M., Recent research and development in titanium alloys for biomedical applications and healthcare goods, *Sci. Technol. Adv. Mater.*, 2003, vol. 4, pp. 445–454.

15. Lee, C.M., Ju, C.P., and Lin, J.H. Chern, Structure-property relationship of cast Ti–Nb alloys, *J. Oral Rehabilit.*, 2002, vol. 29, pp. 314–322.

16. Kollerov, M.Yu., Il'in, A.A., and Skvortsova, S.V., Effect of system and degree of alloying on the characteristics of shape memory effect of titanium alloys, *Metally*, 2001, no. 2, pp. 74–78.

17. Sheremetev, V.A., Prokoshkin, S.D., Brailovskii, V., Dubinskii, S.M., Korotitskii, A.V., Filonov, S.M., and Petrzhik, M.I., Investigation of the structure stability and superelastic behavior of thermomechanically treated Ti–Nb–Zr and Ti–Nb–Ta shape-memory alloys, *Phys. Met. Metallogr.*, 2015, vol. 116, no. 4, pp. 413–422.

18. Konopatskii, A.S., Zhukova, Yu.S., Dubinskii, S.M., Korobkova, A.A., Filonov, M.P., and Prokoshkin, S.D., Microstructure of superplastic alloys based on Ti–Nb for medical purposes, *Metallurgist*, 2016, vol. 60, pp. 223–228.

19. Niinomi, M., Metallic biomaterials, *Jap. Soc. Artif. Org.*, 2008, vol. 11, no. 3, pp. 105–110.

20. Sakaguchi, N., Niinomi, M., Akahori, T., Takeda, J., Toda, H., Relationships between tensile deformation behavior and microstructure in Ti–Nb–Ta–Zr system alloys, *Mater. Sci. Eng. C*, 2005, no. 25, pp. 363–369.

21. Conzalez, M., Pena, J., Manero, J.M., Arciniegas, M., and Gil, F.J., Design and characterization of new Ti–Nb–Hf alloys, *J. Mater. Eng. Perform.*, 2009, vol. 18 (5–6), pp. 490–495.

22. Nitta, K., Watanabe, S., and Masahashi, N., Ni-free Ti–Nb–Sn shape memory alloys, in: *Structural biomaterials for the 21 century*, New Orleans: TMS, 2001, pp. 25–34.

23. Kawashima, A., Watanabe, S., Asami, K., and Hanada, S., XPS study of corrosion behavior of Ti–18Nb–4Sn shape memory alloy in a 0.05 mass % HCl solution, *Mater. Trans.*, 2003, vol. 44, no. 7, pp. 1405–1411.

24. Kolobov, Yu.R., Valiev, R.Z., and Grabovetskaya, G.P., *Grain-Boundary Diffusion and Properties of Nanostructured Materials*, UK: Cambridge Int. Science, 2007.

25. Kolobov, Yu.R., Lipnitskii, A.G., Ivanov, M.B., and Golosov, E.V., Role of the diffusion-controlled processes in the formation of structure and properties of metallic materials, *Compos. Nanostr.*, 2009, no. 2, pp. 5–24.

26. Andrievskii, R.A. and Glezer, A.M., Strength of nanostructures, *Usp. Fiz. Nauk,* 2009, vol. 179, no. 4, pp. 337–358.

27. Dubinskiy, S., Brailovski, V., Prokoshkin, S., Pushin V., Inaekyan, K., Sheremetyev, V., Petrzhik, M., and Filonov, M., Structure and properties of Ti–19.7Nb–5.8Ta shape memory alloy subjected to thermomechanical processing including aging, *J. Mater. Eng. Perform.*, 2013, vol. 22, no. 9, pp. 2656–2664.

28. Hao, Y.L., Zhang, Z.B., Li, S.J., and Yang, R., Microstructure and mechanical behavior of a Ti–24Nb–4Zr–8Sn alloy processed by warm swaging and warm rolling, *Acta Mater.*, 2012, vol. 60, pp. 2169–2177.

29. Václavová, K., Stráský, J., Veselý, J., Gatina, S., Polyakova, V., Semenova, I., and Janeček, M., Evolution of microstructure and microhardness in Ti–15Mo β-Ti alloy prepared by high pressure torsion, *Mater. Sci. Forum.*, 2016, vol. 879, no. 9, pp. 2555–2560.

30. Gatina, S., Semenova, I., Leuthold, J., and Valiev, R., Nanostructuring and phase transformations in the

β-Alloy Ti−15Mo during high-pressure torsion, *Adv. Eng. Mater.*, 2015, vol. 17, no. 12, pp. 1742−1747.

31. Janeček, M., Čížek, J., Stráský, J., Václavová, K., Hruška, P., Polyakova, V., Gatina, S., and Semenova, I., Microstructure evolution in solution treated Ti15Mo alloy processed by high pressure torsion, *Mater. Charact.*, 2014, vol. 98, pp. 233−240.

32. Yilmazer, H., Niinomi, M., Nakai, M., Cho, K., Hieda, J., Todaka, Y., and Miyazaki, T., Mechanical properties of a medical β-type titanium alloy with specific microstructural evolution through high-pressure torsion, *Mater. Sci. Eng. C*, 2013, vol. 33, pp. 2499−2507.

33. Golosova, O.A., Ivanov, M.B., Vershinina, T.N., and Kolobov, Yu.R., Structure and properties of low modulus titanium alloy Ti−26Nb−7Mo−12Zr, *Mater. Sci. Technol.*, 2013, vol. 29, no. 2, pp. 204−209.

34. Betekhtin, V.I., Kolobov, Yu.R., Golosova, O.A., Kardashev, B.K., Kadomtsev, A.G., Narykova, M.V., Ivanov, M.B., and Vershinina, T.N., Elastoplastic proper-ties of a low-modulus titanium-based β alloy, *Technical Phys.*, 2013, vol. 58, no. 10, pp. 1432−1436.

35. Betekhtin, V.I., Kolobov, Yu.R., Golosova, O.A., Dvorak, J., Sklenicka, V., Kardashev, B.K., Kadomtsev, A.G., Narykova, M.V., and Ivanov, M.B., Elastic modulus, microplastic properties and durability of titanium alloys for biomedical applications, *Rev. Adv. Mater. Sci.*, 2016, vol. 45, no. 1/2, pp. 42−51.

36. Kydryashov, S.I., Golosova, O.A., Kolobova, A.Yu., Kolobov, Yu.R., and Golosov, E.V., Comparative investigation of the features of the nanostructuring surface relief of α- and β-titanium alloys at pulsed femto-second laser irradiation, *Compoz. Nanostr.*, 2014, vol. 6, no. 3, pp. 2−11.

37. Kolobov, Yu.R., Golosov, E.V., Ratochka, I.V. Features of submicrocrystalline structure and its effect on mechanical properties of titanium alloys, *Vopr. Materialoved.*, 2008, vol. 2, no. 54, pp. 43−50.

Translated by O. Golosova